Proc. of the 9th International Symposium on Geotechnical Safety and Risk (ISGSR)
Edited by Zhongqiang Liu, Jian Dai and Kate Robinson
Published by Research Publishing, Singapore. ©2025 The Author(s), CC-BY 4.0 licence.
doi: 10.3850/GRF-25280825_isgsr-214-P185-cd

INVESTIGATION OF THE IMPACT OF GEOLOGICAL UNCERTAINTY ON THE RISK OF SUBSEA TUNNEL CROSSING A FAULT ZONE

Jiaze Ni

Department of Geotechnical Engineering, Tongji University, China. E-mail: nijz@tongji.edu.cn

Jinzhang Zhang

Department of Civil and Environmental Engineering, The Hong Kong University of Science and Technology, China. E-mail: zhangjz@ust.hk

Le Zhang

Qingdao Guoxin Jiaozhou Bay Second Submarine Tunnel Co., Ltd, China. E-mail: lezhang2017@126.com

Hongwei Huang

Department of Geotechnical Engineering, Tongji University, China. E-mail: huanghw@tongji.edu.cn

Abstract: Subsea tunnels crossing fault zones face significant uncertainties in various parameters, which pose substantial adverse effects on excavation risks. In this paper. firstly, a statistical analysis of six parameters in the fault zones of the Qingdao Jiaozhou Bay Second Subsea Tunnel (hereinafter referred to as "Qingdao Second Tunnel")was conducted, including seawater depth, tunnel burial depth, surrounding rock unit weight, elastic modulus, cohesion, and friction angle. Then, comprehensive load index and resistance index were proposed to quantitatively evaluate the magnitude and uncertainty of load and resistance. Meanwhile, their distributions and correlations were also examined.Subsequently, reliability analysis was carried out via a Kriging-based Response Surface Method (RSM) using a 3D numerical model validatedwith field data. Results indicate that the failure probability of the Qingdao Second Tunnel crossing fault zonesis0.3%.Finally, five risk grades were divided based on the maximum crown settlementof tunnel, which can be referenced in engineering risk management.

Keywords: Subsea tunnel, Fault zone, Kriging-based RSM, Risk, Reliability analysis, Distribution, Correlation.

1. Introduction

Fault zones, due to their complex geological structures, exhibit extremely high uncertainty in stratigraphic distribution and geotechnical parameters. Moreover, when a subsea tunnel crosses fault zones, the infinite supply of overlying seawater further increases the loads exerted on the tunnel. Therefore, exploring the impact of geotechnical uncertainties on the risks associated with a subsea tunnel crossing fault zones holds significant scientific research value and engineering application importance.

Many scholars have studied the influencing factors and their effects on tunnels crossing fault zones.Kiani et al. (2016) and Sabagh et al. (2020) investigated the impact of tunnel cover thickness, fault angle, tunnel diameter, and lining thickness on the stability of surrounding rocks when crossing through fault zones. Li et al. (2023) identified three typical failure modes when crossing fault zones in tunnel face excavation.Zaheri et al. (2020) conducted a 3D numerical simulation study on the interaction between tunnel linings and strike-slip faults, exploring the influence of mechanical properties of soils, tunnel layer thickness, tunnel depth, fault dip angle, and their impact on tunnel mechanical performance.However, few scholars have conducted reliability analysis for subsea tunnels crossing fault zones, considering the uncertainties in load and resistance.

Based on the Qingdao Second Tunnel, which crosses 10 fault zones over its total length of 1,970 meters, this study first collects statistical data on the tunnel's burial depth and seawater depth at every meter along its alignment. By interpolating geological survey data, the elastic modulus, cohesion, and friction angle of the surrounding rock at every meter of the tunnel's length are determined. Using these data, the distribution of loads and resistances, as well as their correlations, are analyzed. Subsequently, a verified3D numerical model is employed, and reliability analysis of the Qingdao Second Tunnel crossing a fault zone is conducted using load and resistance as independent variables through the Kriging-basedRSM.

2.Parameter distribution and correlation in Qingdao Second Tunnel

Data for each meter along the 1,970m marine section of the Qingdao Second Tunnel crossing 10 fault zones were collected. The data consist of seawater depthd_s, tunnel burial depthd_r, unit weight$^3{}_r$, elastic modulus$E$, cohesion$c$, and friction angle$Æ$ Based on these data, the distribution of each parameter and their mutual correlations will be first analysed in this section. Subsequently, these parameters are combined into two indexes representing load and resistance, respectively. The distributions and correlations of these coefficients are derived to serve as the basis for the reliability analysis in section 3.

2.1.*Distribution and correlation of basic parameters*

The distributions and correlations of above six parameters in the fault zones of the Qingdao Second Tunnel marine section are shown in Fig. 1. From the figure, it can be observed that sea depth, burial depth, and surrounding rock unit weight approximately follow normal distributions. Their mean values are 25.798 m, 63.831 m, and 25.470 kN/m³, respectively, with coefficients of variation of 0.456, 0.135, and 0.015.

In contrast, the three mechanical parameters of the surrounding rock—*E*, *c*, and *Æ*—exhibit a tendency for peak values to occur at higher magnitudes. This is primarily because ⑦$_9$ slightly weathered granite dominates, being the most prevalent surrounding rock type in the marine section of the Qingdao Second Tunnel, and it has relatively high mechanical parameter values. After appropriate transformation, these three mechanical parameters can be approximated as following log-normal distributions. Their mean values are 23,237.462 MPa, 4,912.355 kPa, and 30.289°, with coefficients of variation of 0.342, 0.461, and 0.165, respectively.

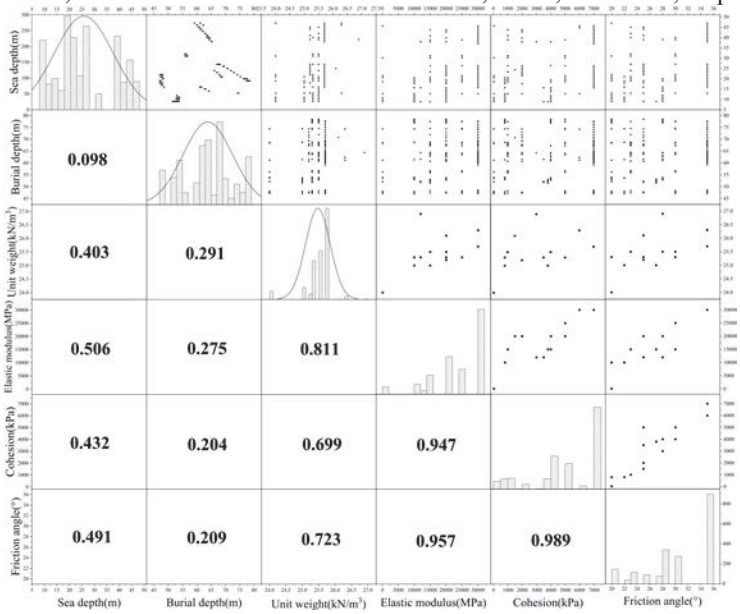

Fig. 1.Distribution and correlation of six basic parameters

2.2.*Distribution of load and resistanceindex and their correlation*

To reduce the dimension of the Kriging-based Response Surface Method (RSM) input variables and improve its computational efficiency, the six parameters mentioned above are grouped into two categories: load and resistance. The comprehensive load index and resistance index are calculated using Eq.(1) and Eq.(2), respectively.

The load index*L* is represented by sea depthd_s, tunnel burial depthd_r, and the unit weight of the surrounding rock³$_r$. A larger comprehensive load index indicates that the tunnel is subjected to greater overlying loads.

$$L = \gamma_s d_s + \gamma_r d_r , \tag{1}$$

where ³$_s$ denotes the unit weight of seawater, which is 10 kN/m^3 here.

The resistance index is represented by the elastic modulus, cohesion, and friction angle of the surrounding rock.Since these three mechanical parameters approximate log-normal distributions after transformation, the comprehensive resistance index is defined in the form of a product.After taking the logarithm of the resistance index, it appears as the sum of the three normal distribution parameters, that is, it still follows the lognormal distribution, which is convenient for the sampling process of reliability analysis.A smaller comprehensive resistance index suggests that the surrounding rock has a stronger ability to resist deformation under external forces.

$$R = \prod_{i=E,c,\varphi} (\max_i + \frac{1}{3}\sigma_i - i)^{\alpha_i} , \tag{2}$$

where max$_i$is the maximum of one of these three parameters; $\tilde{A}_i$is the standard deviation of one of these three parameters;±$_i$is the weight of each parameter, satisfying $\sum_i \alpha_i = 1$, here ±$_E$=0.6, ±$_c$=0.3, and ±$_{\bar{Æ}}$=0.1, to emphasize the importance of stiffness (elastic modulus)for in this project, tunnel deformation is used to evaluate the risk.

The load index, resistance index, and their correlation are shown in Figures 2 to 4. The comprehensive load index approximately follows a normal distribution with a mean of 1,884.674 kPa and a standard deviation of 268.670 kPa. The comprehensive resistance index approximately follows a log-normal distribution with a mean of 7.690 and a standard deviation of 0.882. The two indices exhibit a negative correlation, with a correlation coefficient of -0.483.The distributions and correlations described above will serve as the fundamental input data for the reliability analysis in the next chapter.

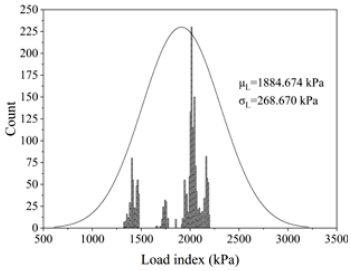

Fig. 2.Distribution of load index

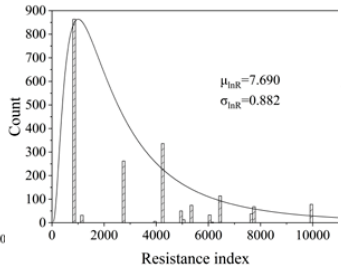

Fig. 3.Distribution of resistance index

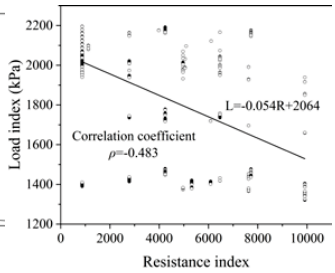

Fig. 4.Correlation of two indexes

3. Reliability analysis withKriging-basedRSM

Based on the parameter distributions and correlations obtained in thesection 2, a Kriging-based response surface will be constructed usinga validated 3D numerical model to conduct reliability analysis.

3.1.*Verified 3D numerical model of subsea tunnel crossing a fault zone*

To obtain the inputdata required for constructing the response surface, a 3D numerical model of the Qingdao Second Tunnel crossing the f10 fault zone was developed using FLAC 3D, as shown in Fig. 5. In this model, the surrounding rock is modelled using the Mohr-Coulomb constitutive model, with parameters listed in Table 1. The tunnel lining is simulated withLiner structural elements, while rock bolts are simulated withCable elements. The arrangement of the initial lining is based on the construction design drawings.

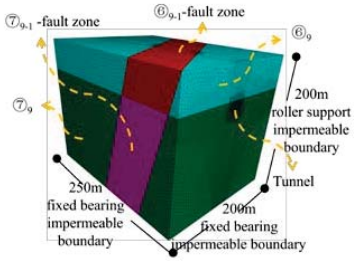

Fig. 5.Numerical model

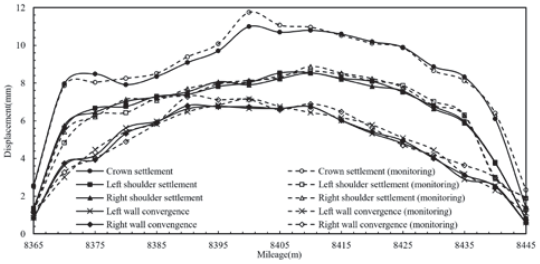

Fig. 6.Validation of numerical model

Table 1. The parameters of the surrounding rock in the numerical model

Parameters	⑥$_9$Moderately weathered granite	⑦$_9$Slightly weathered granite	⑥$_{9\text{-}1}$Moderately weathered fractured granite	⑦$_{9\text{-}1}$Slightly weathered fractured granite
Bulk modulus/GPa	27.78	25	50	33.33
Shear modulus/GPa	9.26	11.54	5.17	7.14
Cohesion/kPa	0.5	0.7	0.1	0.12
Friction angle/°	30	35	20	25
Extension strength/MPa	0	0	0	0
Dry density/kg·m^{-3}	1530	1570	1550	1520
Porosity	0.01	0.005	0.04	0.02
Permeability coefficient/m^3·s·kg^{-1}	3.54×10^{-12}	5.91×10^{-12}	2.36×10^{-10}	3.54×10^{-10}

The deformations of the tunnel crown, left and right arch shoulders, and left and right sidewalls was compared with monitoring data, as shown in Fig. 6. The comparison indicates good agreement between the simulation results and the monitoring data, demonstrating that the model can effectively simulate the deformation behaviour of the tunnel crossing a fault zone.

3.2.*Construction of response surface and reliability analysis*

Based on the distributions and parameters of the load index and resistance index obtained in Section 2.2, 80 sets of L and R were generated using the Latin Hypercube Sampling (LHS)method. These data were converted into the corresponding rock unit weight and three mechanical parameters, which were subsequently input into the numerical model to calculate the maximum crown settlement for each of the 80 cases. The resulting 80 sets of independent variables (L, R) and dependent variables (settlement) were then used as inputs to train the Kriging response surface model.

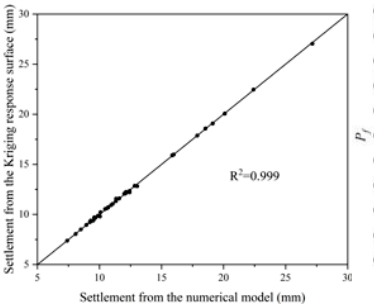

Fig. 7.Validation of the RSM

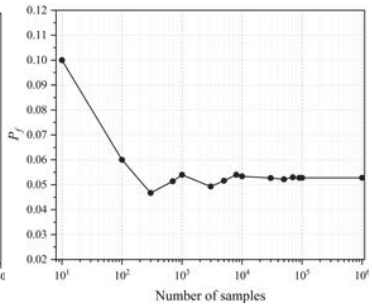

Fig. 8.Variation of P_f with sample size

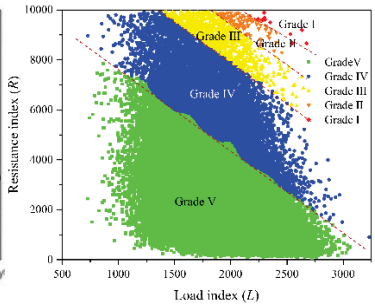

Fig.9. Risk grade divided by L and R

After training, 40 additional sets of *L* and *R* were generated using LHS. The maximum settlements calculated using the Kriging response surface and the numerical model were compared, as shown in Fig. 7, and the accuracy of the response surface was verified.Subsequently, assuming a structural failure criterion where the maximum crown settlement exceeds 20 mm (refer to JTG/T 3660-2020), the failure probability P_f was calculated.Its trend with increasing Monte Carlo simulation sample size was analyzed, as shown in Fig. 8. It was observed that when the sample size exceeds 10^4, the results become stable near 5.28%.

Using LHS, 10^4 sets of *L* and *R* were generated and input into the response surface for computation. Based on the probability of maximum relativetunnel crown settlement, five risk levels were defined, as detailed in Table 2. These levels can serve as a reference for engineering risk warning and emergency measure formulation.

Table 2. The risk grades divided by maximum relative crown settlement

Risk Grade	Ⅰ	Ⅱ	Ⅲ	Ⅳ	Ⅴ
Probability	0.001%	0.01%	0.1%	1%	10%
Relative deformation	e0.17%H	0.15%~0.17%H	0.13%~0.15%H	0.09%~0.13%H	<0.09%H

Note: H is the tunnel section height.

Finally, 10^5 sets of datawere input into the response surface for computation. The results were categorized into five risk levels in Table 2, as shown in Fig. 9. Prior to tunnel excavation, the settlement risk level at a specific mileage can be predicted using prior information (e.g., geological survey data) to calculate *L* and *R* and referencing Fig. 9. This approach facilitates proactive risk management before tunnel excavation.

4. Conclusions

This study investigated the impact of geotechnical parameter uncertainties on the risk of subsea tunnel crossing fault zones through mathematical statistics, numerical simulation, and reliability analysis. Thefollowing conclusions are reached in this study:

(1) Anormal load index and a log-normal resistance index were proposed, which effectively capture the magnitude and uncertainty of load and resistance for subsea tunnels crossing fault zones.

(2) Thefailure probability of the Qingdao Second Tunnel's marine section crossing fault zones is 5.28%.

(3) The maximum relative tunnel crown settlementis categorized into five risk grades, which can be predicted using the response surface based on *L* and *R*.

Acknowledgement

This study is supported by the Natural Science Foundation Committee Program of China (No. 52130805, 52408434),the Shanghai Pujiang Program (2022PJD077)and the Research and Consultation on Comprehensive Risk Management of the Second Jiaozhou Bay Tunnel Project (No. ESJH-ZB-069).

References

Kiani, M., Akhlaghi, T., Ghalandarzadeh, A. (2016). Experimental modeling of segmental shallow tunnels in alluvial affected by normal faults. *Tunnelling and Underground Space Technology*, 51, 108-119.

Li, Z. Y., Huang, H. W., Zhou, M. L., et al.(2023). Failure responses of rock tunnel faces during excavation through the fault-fracture zone. *Underground Space*, 10, 166-181.

Sabagh, M., Ghalandarzadeh, A. (2020). Numerical modelings of continuous shallow tunnels subject to reverse faulting and its verification through a centrifuge. *Computers and Geotechnics*, 128, 103813.

Zaheri, M., Ranjbarnia, M., Dias, D., et al.(2020). Performance of segmental and shotcrete linings in shallow tunnels crossing a transverse strike-slip faulting. *Transportation Geotechnics*, 23, 100333.

Zhang, J., Xiao, T., Ji, J., et al. (2021). *Geotechnical reliability analysis: theories, methods, and algorithms*. Tongji University Press.

China Communications First Public Bureau Group Co., LTD. (2020). *Technical Specifications for Construction of Highway Tunnel*. JTG/T 3660-2020.